BNL-224196-2023-TECH

NSRL-TN-23-001

Muon Decay Study at NSRL

J. Gasparik

March 2023

Collider Accelerator Department

Brookhaven National Laboratory

U.S. Department of Energy

USDOE Office of Science (SC), Nuclear Physics (NP) (SC-26)

DISCLAIMER

Muon Decay Study at NSRL

March 3, 2023

1 Introduction

A muon is an unstable subatomic particle, classified as a lepton according to the Standard Model. Muons are charged leptons with 1/2 spin. They were discovered by Neddermeyer and Anderson [1937] from hadronic cosmic ray showers. Figure 1 provides a visual representation of a cosmic ray shower in Earth's atmosphere. At a height of 50 000 m in the atmosphere, a primary cosmic ray (mainly protons, helium, a heavy nucleus or a gamma ray) interacts with a gas molecule. The striking of a gas molecule creates a cosmic ray shower, where the energy of the primary particle is distributed among many secondary particles and gamma rays. With each interaction, the cosmic ray particles in the shower lose energy but distribute this energy among a higher number of particles. From the initial interaction, primarily heavy nuclei and pions are generated. Heavy nuclei will interact with gas molecules to produce protons, gamma rays, electrons and pions. The dominant decay mode of neutral pions is to two gamma rays, while charged pions decay to a muon and a neutrino (equation 1).

$$\begin{aligned} \pi^+ &\rightarrow \mu^+ + \nu_\mu \\ \pi^- &\rightarrow \mu^- + \overline{\nu}_\mu \end{aligned} \tag{1}$$

As pictured in Figure 1, muons comprise the majority of cosmic ray particles reaching the surface of the Earth. For perspective, every cell in the human body (all 37.2 trillion of them) gets hit by a muon every year. Our bodies are constantly being hit by muons, and our cells have excellent repair mechanisms for muon damage. Muons travel at nearly the speed of light, meaning they are subject to relativistic effects. The time dilation effect allows secondary muon cosmic rays to penetrate the atmosphere and reach Earth's surface before decaying.

The experimental value of the muon lifetime is highly studied. The free decay literature value is $\tau = 2.197\,03\,\mu$s [Kuno and Okada, 2001]. However, this lifetime can vary depending on the material where the decay occurs and the muon charge [Bahmanabadi et al., 2005, 2006]. Several studies [Bahmanabadi et al., 2005, 2006, Khachatryan and Collaboration, 2010] found the positive to negative charge ratio to be ≈1.2-1.3, meaning there are slightly more positive muons than negative. The lifetime of positive muons is independent of material where the decay occurs, while the lifetime of negative muons varies depending of the atomic number Z of the material. The lifetime of negative muons will decrease as the Z of the decay material increases. Meaning our experimental setup should measure a lifetime slightly lower than the published value. Since we do not know the exact lifetime of a negative muon in our experimental materials, nor do we know the exact positive to negative muon charge ratio during the experiment, the literature value will be designated as truth. However, given the experimental setup it is likely the lifetime will be slightly lower than literature.

The goal of this experiment was the verify the muon lifetime using a scintillator at the NASA Space Radiation Lab (NSRL) located at Brookhaven National Laboratory. Upon contacting the

scintillator at NSRL, there is a potential for the muon to decay within the scintillator itself. This would provide two scintillator signals: (1) from the initial muon impact, and (2) from the electron produced in the muon decay. The positive (μ^+) and negative muon (μ^-) decay are seen in equation 2 [Kuno and Okada, 2001]. Though these decay mechanisms cannot be distinguished [Kuno and Okada, 2001], the resulting electron from muon decay can be detected in the NSRL scintillator. Further information on experimental setup is discussed in the following section. This experiment serves to measure muon lifetime while gaining experience with the NSRL's new CAEN DT5730S data acquisition (DAQ) system.

$$\begin{aligned} \mu^+ &\rightarrow e^+ + \nu_e + \overline{\nu}_\mu \\ \mu^- &\rightarrow e^- + \overline{\nu}_e + \nu_\mu \end{aligned} \tag{2}$$

2 Experimental Setup

The muon and muon decay signal were measured using an 15 cm x 10 cm x 12.6 cm scintillator. The height of this scintillator provides sufficient physical space for the decay to occur within the scintillator. The digital signals at each step of the experimental setup are pictures in Figures 2-4. Capturing signals occurring at $> 2\,\mu$s required a long gate signal, after the initial muon signal, to be in coincidence with the electron signal. To elaborate, the raw scintillator signal is sent to a discriminator, whose output is seen in Figure 2(1). The initial galactic cosmic ray muon pulse is in black, while the grey pulse represents the reflection from the scintillator signal. One option to remove this reflection signal is raising the discriminator threshold. However, considering muon signals may be relatively small, raising the discriminator threshold may also unintentionally remove the muon signals. Since raising the discriminator threshold is not an option in this experiment, a logic setup was designed to "ignore" the reflection. To measure the muon exponential decay pattern the initial muon pulse is elongated to 100 μs using a gate generator (Figure 2(2)). Then the gated signal delayed by 200 ns (Figure 2(3)). Creating a long delayed signal provided a window to capture muon decay electron pulses. This signal was then split, with one output going to a discriminator and the other going to a coincidence unit. Figure 3 shows the two signals going to the coincidence unit, one of them being the delayed gate signal and the other being the discriminated scintillator signal. These signals will only be in coincidence when there is a measurable muon decay. The coincidence signal represents a muon decay product and serves as the second signal in the muon lifetime measurement. The final coincidence signal and the initial discriminated scintillator signal serve as the two inputs to the DAQ system. The time difference between these pulses represents the time between the initial muon pulse, and the pulse from the muon decay. The DAQ was set to measure time of flight.

3 Results

The data collection period spanned five continuous days, with N = 5 581 events collected. The raw data from the DAQ system contains time stamps from the two input pulses. These timestamps were subtracted to calculate the difference in time between the initial muon pulse and the electron pulse from the muon decay. A histogram of 1 μs bin size was constructed with the subtracted pulse times. The histogram counts are plotted in Figure 5 labeled 'data'. The muon decay is fitted to an exponential decay curve (equation 3).

$$C(t) = C_0 e^{\frac{-t}{\tau}} + B \tag{3}$$

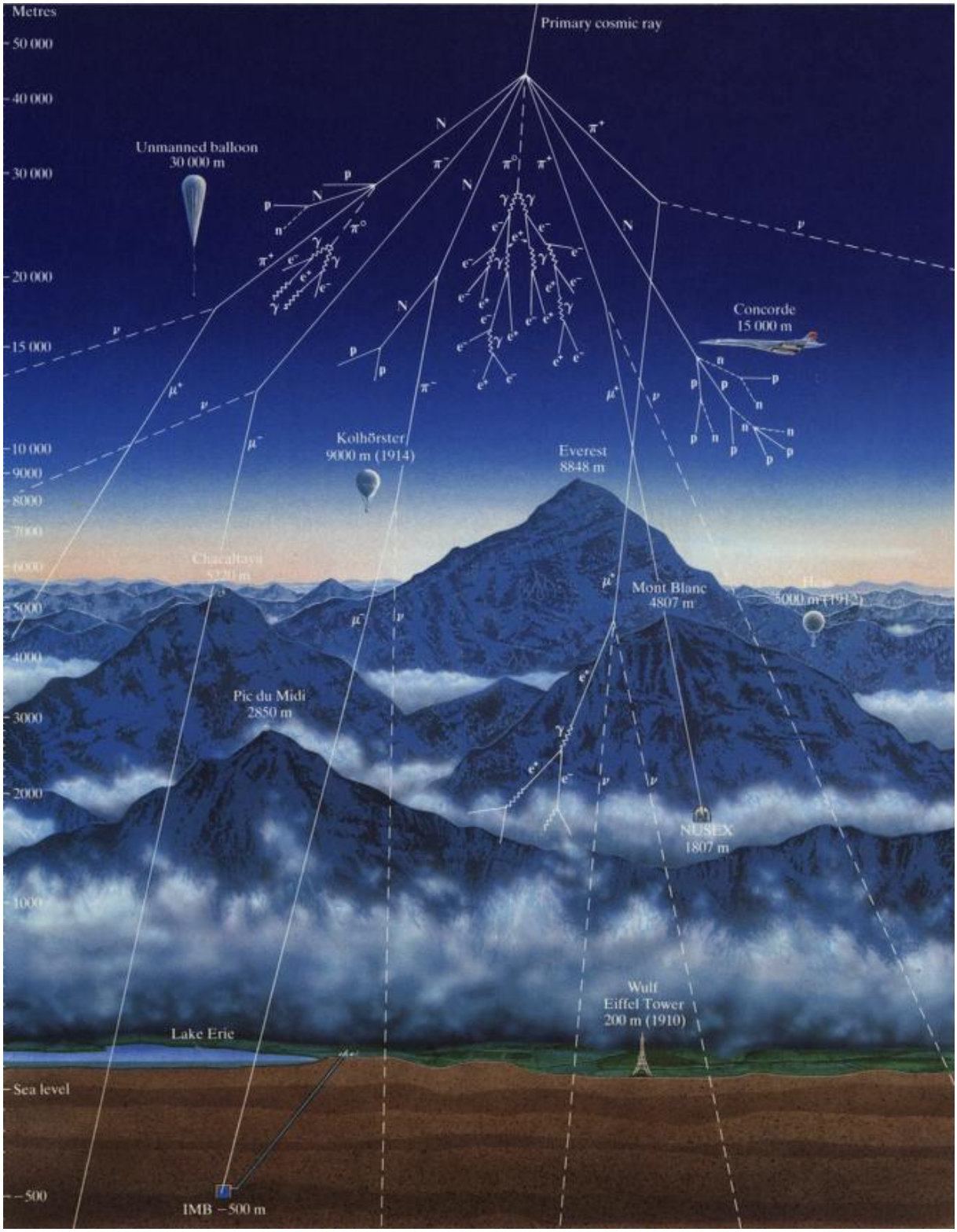

Figure 1: Cosmic ray shower in Earth's atmosphere.
N - nucleus, π - pion, p - proton, n - neutron, e^{-1} - electron, γ - gamma ray, μ - muon, and ν - neutrino

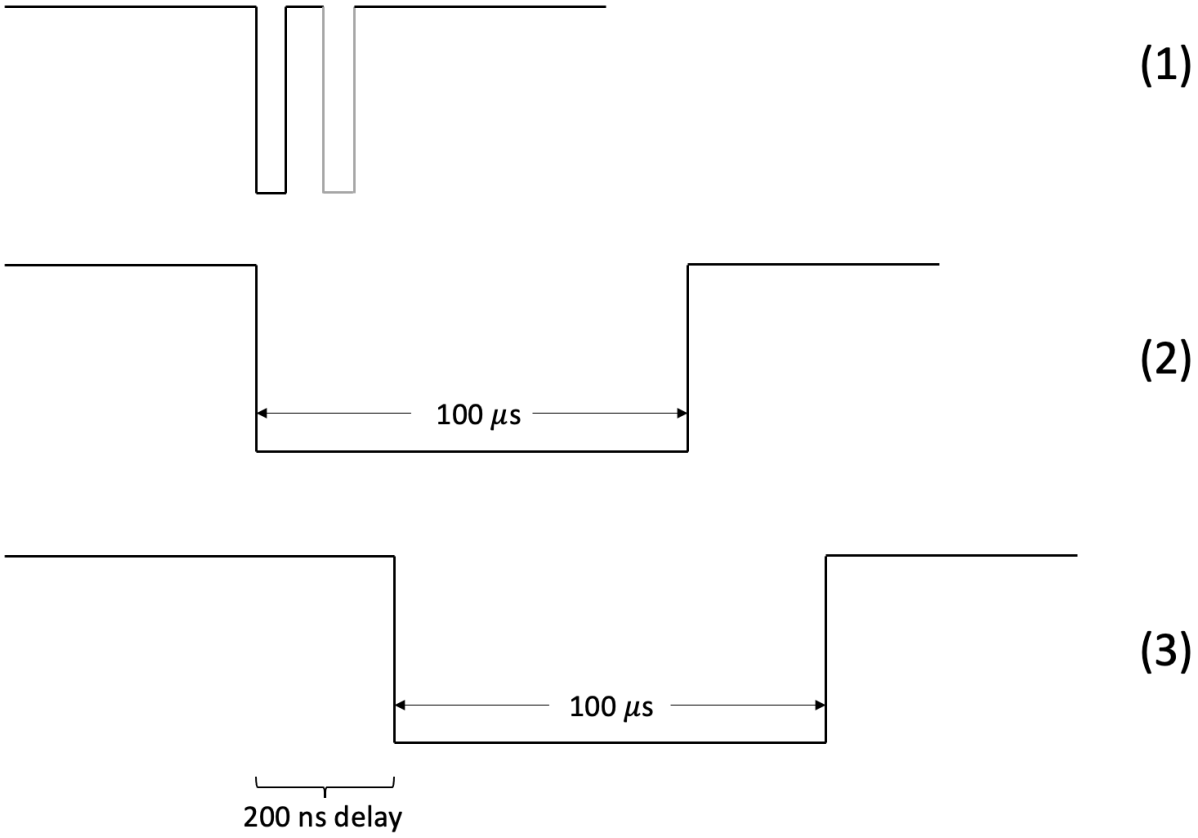

Figure 2: (1) Scintillator signal (after discriminator) showing initial pulse, followed by scintillator signal reflection pulse. (2) Scintillator signal through gate generator to stretch signal to 100 μs. (3) Delay gated signal by 200 ns.

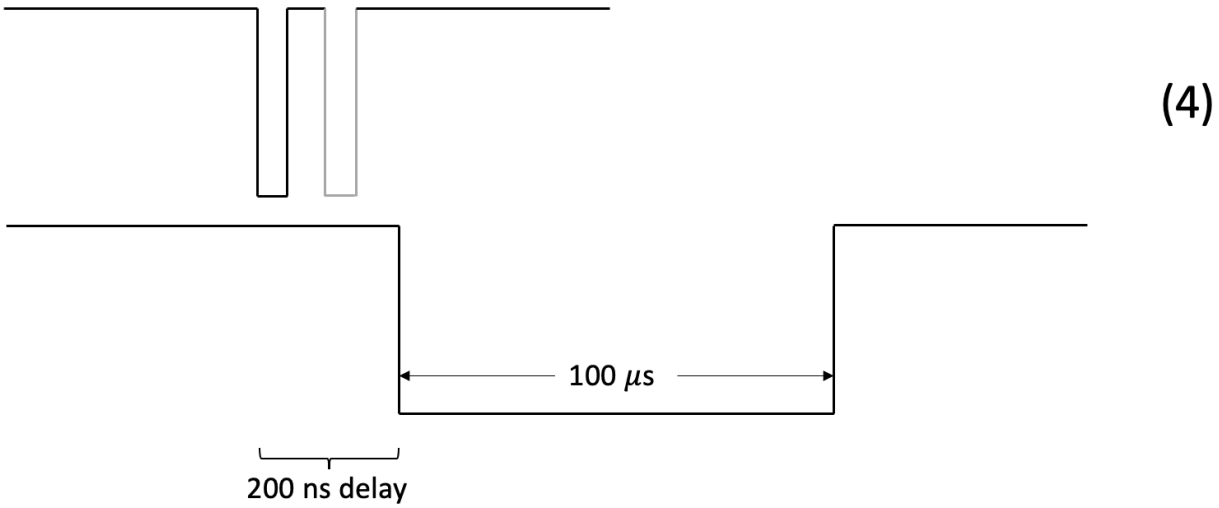

Figure 3: Put discriminated scintillator signal in coincidence with delayed gate signal.

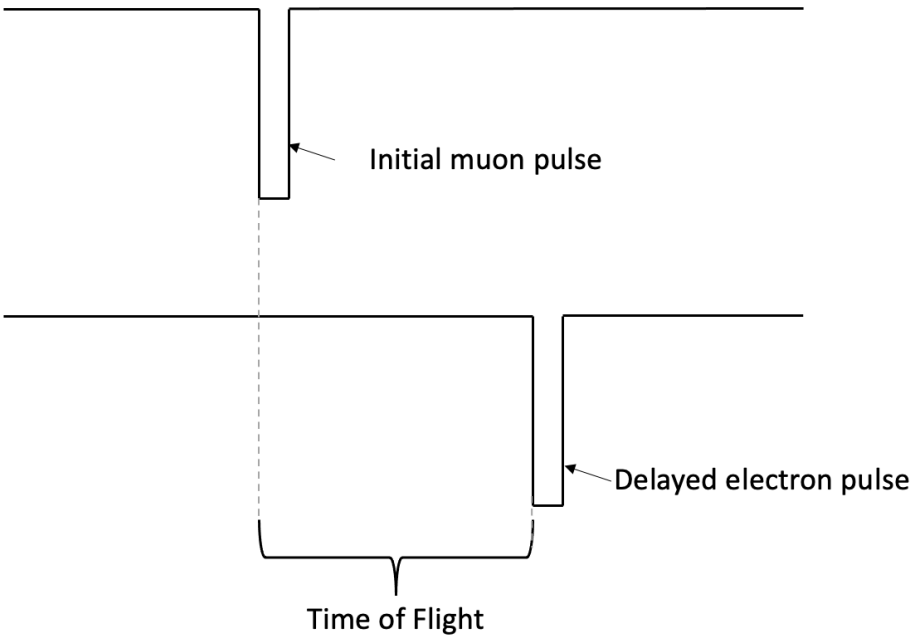

(5)

Figure 4: Two signals sent to DAQ system. Second signal only produced if delayed signal in coincidence with delayed gate.

In equation 3 C is the number of events, C_0 being the number of initial events, t is time, τ is the muon lifetime, and B is the background correction factor. Non-linear least squares method was used to optimize the fit parameters (C_0, τ, and B) seen in the fit in Figure 5. The associated covariance matrix (equation 4) is calculated with the exponential fit. The top plot of Figure 5 shows the histogram data and fit including fit parameters. The error bars are calculated by $\sigma = \sqrt{N_i}$ where N_i is the number of counts (N) in each bin (i). The bottom plot in Figure 5 shows the residuals (Δ_i = observed value - expected value = N_i - C) and the error bars are calculated as $\sqrt{N_i}$ (the same as in the top plot). Based on a non-linear least squares fit method, the calculated $\tau = 2.116 \pm 0.027\,\mu s$. The error on the lifetime is calculated from the square root of the variance of τ, $\sqrt{\sigma_\tau^2}$, or the square root of the middle element of the covariance matrix. The calculated value does not agree with the literature value; however, the lifetime only differs from the literature value by 3.7%. One aspect contributing to the difference in lifetime between our calculated value and the literature value is the composition of the scintillator. Scintillator material contains carbon which will lower the lifetime of the negative muons. As stated in the Introduction section, a slightly lower lifetime than literature was expected due to capture of the μ^- by the C and the H nuclei.

$$\begin{bmatrix} \sigma_{C_0}^2 & \sigma_{C_0\tau} & \sigma_{C_0 B} \\ \sigma_{\tau C_0} & \sigma_\tau^2 & \sigma_{\tau B} \\ \sigma_{B C_0} & \sigma_{B\tau} & \sigma_B^2 \end{bmatrix} \tag{4}$$

Figure 6 is the same as Figure 5 but with the time axis restricted to the decay portion of the curve. Errors decrease as time increases since error is solely a function of the number of counts. The fit agrees with the data.

The χ^2 and the *reduced chi squared* $\tilde{\chi}^2$ are computed using σ and Δ based on equations 5 and 6, respectively. Here d = i - c, where i is the number of bins (i=28) and c is the number of parameters calculated from the data and used in the fit (c=3).

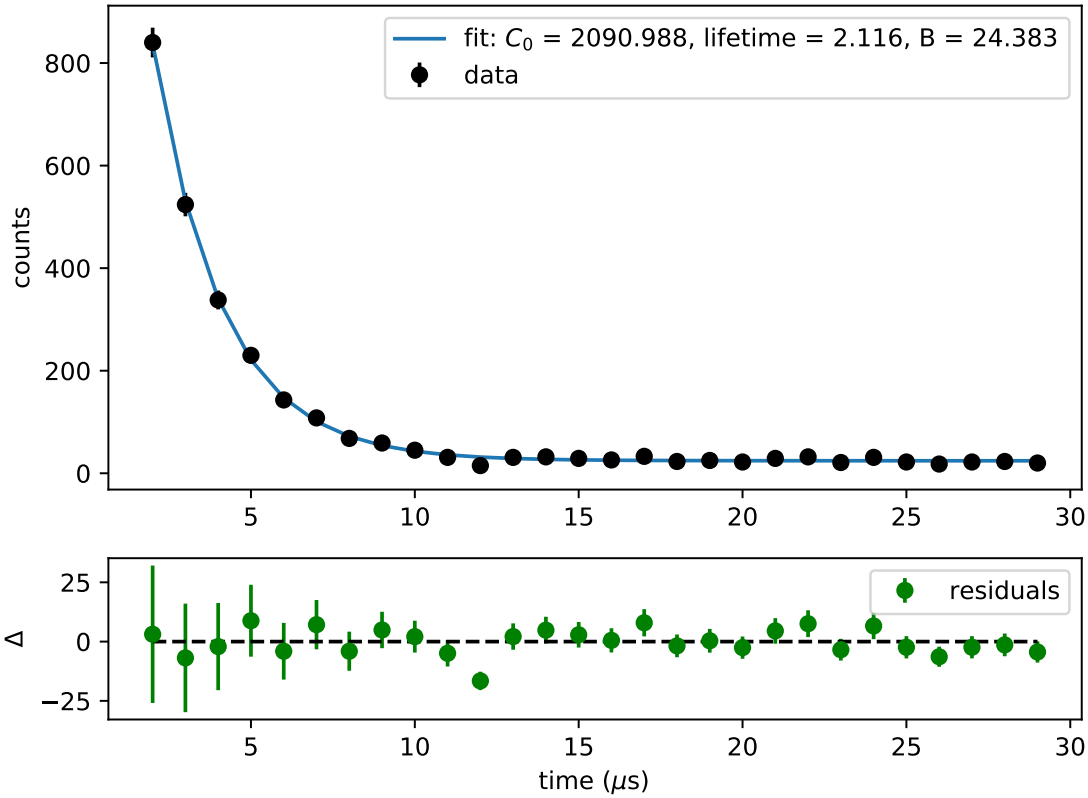

Figure 5: The top plot shows binned data, and least squares fit with fit parameters. Residuals (data - fit) are plotted in the bottom plot. Error bars are $=\sqrt{N_i}$ and the dotted line is plotted at Δ=0.

$$\chi^2 = \sum_i^1 (\frac{\Delta_i}{\sigma_i})^2 \tag{5}$$

$$\tilde{\chi}^2 = \frac{\chi^2}{d} \tag{6}$$

The $\tilde{\chi}^2$ value for the 1 μs bin is 1.308. A value of $\tilde{\chi}^2$ of order one or less means the expected distribution agrees with the observed. The $\tilde{\chi}^2$ value as a function of bins size is explored in the Error Analysis section.

4 Statistical Error Analysis

Thus far, lifetime uncertainty was calculated using the covariance matrix associated with the fit. Two additional and independent methods were used to verify the calculated error: (1) based on repeated iterations and (2) the τ value necessary to increase χ^2 by 1. In more detail, the repeated iterations method required randomly generating 3 000 decay curves, and analyzing the fit parameters. First, at each datapoint in Figure 5 a normal distribution with $\sigma = \sqrt{N_i}$ was constructed. Repeating this process 3 000 times yields 3 000 normally distributed decay curves. Next, the parameters (C_0, τ, and B) were calculated for each decay curve. An average value of C_0 and B are computed from the 3 000 fit parameters calculated. Each decay curve is then fit

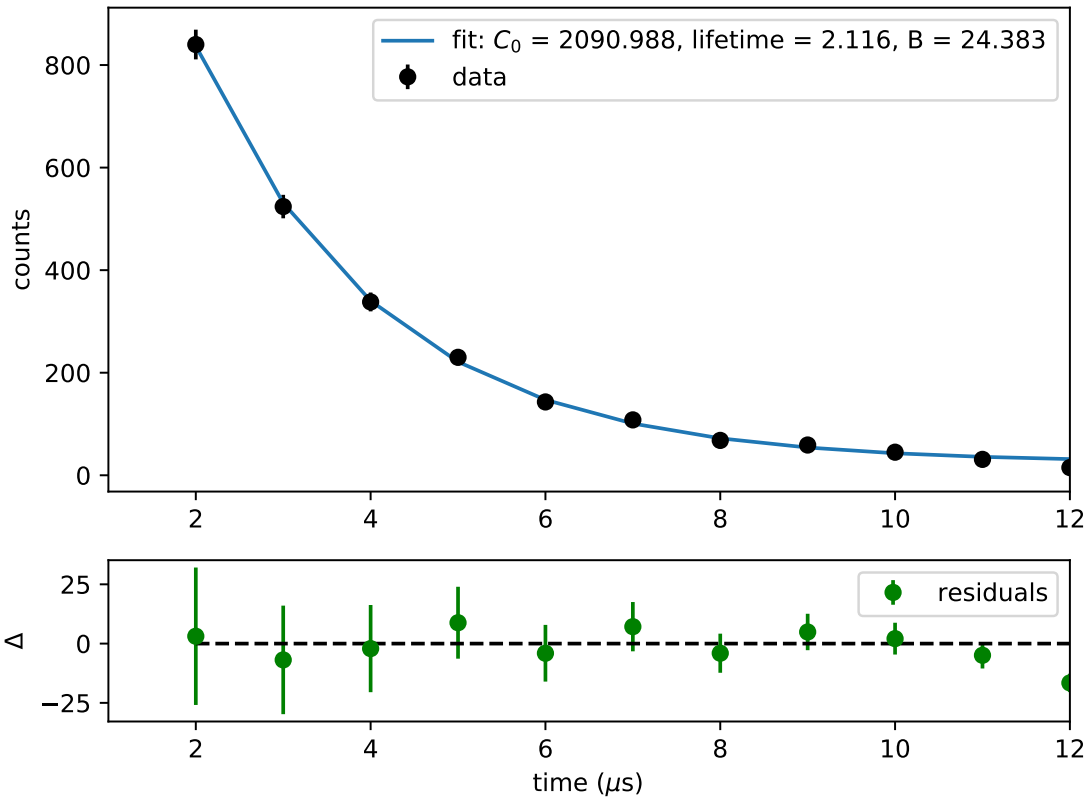

Figure 6: Same as Figure 5 but with restricted time axis (x-axis).

for a second time, but now only τ can vary while C_0 and B remain fixed at their average values. The decay curves with fixed C_0 and B are plotted in Figure 7. The histogram of the computed lifetime values is seen in Figure 8. This distribution has an average lifetime of 2.111 μs with a $\sigma = 0.034$ μs. Since the 3 000 decay curves are randomly generated, these numbers can change slightly.

The second independent error method required changing the value of τ, and recording where χ^2 changed by a value of 1. This method was conducted using trial and error to yield a value of $\tau = 2.116 \pm 0.020\,\mu s$.

In summary, the three independent error analysis methods ($\sqrt{\sigma_\tau^2}$, repeated trials, and changing χ^2 by 1) yield three different values for the error on τ: 0.027 μs, 0.034 μs, and 0.020 μs. The calculated lifetime and error from the iterations method can yield slight differences in the values from run to run. The iterations method yields the highest error, while changing χ^2 by 1 yields the smallest. The calculated value from the square root of σ_τ^2 is exactly between the two error extremes from the other two methods. None of the methods produce results which agree with the literature value; though, these differences are attributed to the reduced decay time of negative muons in scintillator materials. The $\sqrt{\sigma_\tau^2}$ method is used in the remainder of this paper.

5 Experimental Reproducibility and "Choices"

The experimental setup to measure muon decays consisted of a scintillator, logic setup and DAQ system. Statistical and human errors were minimal and most errors can be attributed to

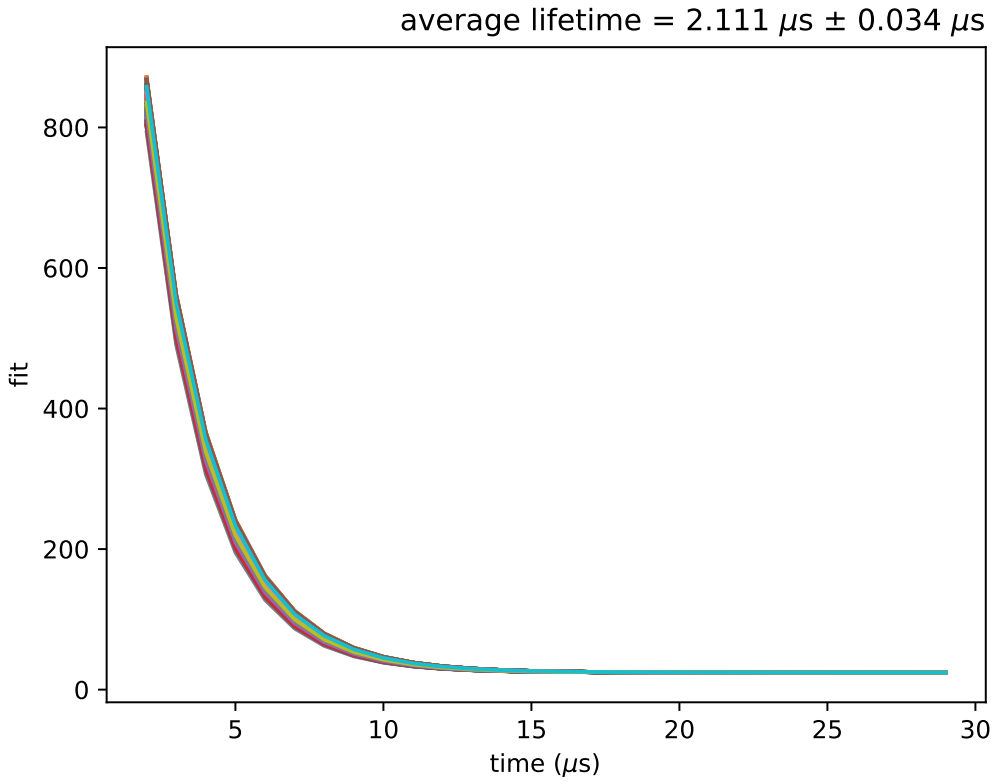

Figure 7: Normally distributed decay curves fitted with fixed values of C_0 and B. The average lifetime $\pm\sigma$ is indicated. There are 3 000 decay curves in total. The approximate values of C_0 and B are 2 095.87 $\pm$ 133.66 counts and 24.41 $\pm$ 1.48 counts, respectively.

systematic errors. Systematic errors encompass predetermined errors within the experimental equipment including scintillator and DAQ limitations. Systematic errors are not explicitly discussed in this report. Instead, the reproducibility of the experiment is analyzed. Specifically, the experiment was repeated a second time to study statistical errors associated with the measurement. Data collection and analysis procedures were identical between the two experimental periods. Several choices were made during the analysis of the initial dataset which intentionally remained consistent in the analysis of the second dataset. Within the analysis there are several choices made which significantly alter the lifetime calculation. The following paragraph elaborates on this. All of the choices were justified and remained the same in the analysis of the second dataset. This procedure mitigated the human bias associated with attempting to perfectly replicate a known literature value.

The data presented in the Results section were collected from September 15-20, 2022. An initial dataset was collected September 1-6, 2022 with the preliminary analysis performed on this dataset. The September 1st-6th dataset consisted of 4 775 datapoints. The first step in the analysis is to subtract channel 1 (CH1) - channel 0 (CH0), corresponding to the initial discriminated muon pulse (CH1 in the DAQ) and the coincidence decay pulse (CH0 in the DAQ). This calculation yields the time between pulses in μs. Next, the time between pulses is binned and plotted revealing the muon decay curve (data values in top plot of Figure 5). The first choice made in the analysis was the size of the bins. Thus far, a 1 μs bin size, was used throughout the Results section. Later on in the error analysis there is a discussion on

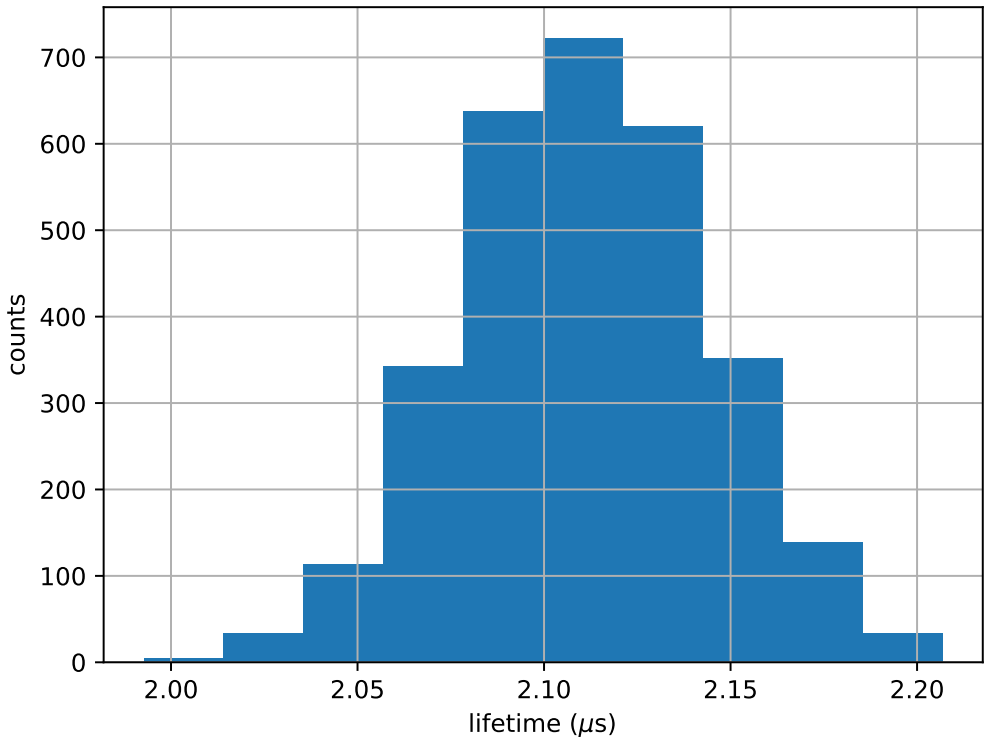

Figure 8: Histogram of computed lifetime values. The distribution has an average lifetime of 2.111 μs and a $\sigma = 0.034$ μs.

consequences of changing bin width in relation to the lifetime and $\tilde{\chi}^2$ value. The second choice made was the length of the bin array. Our maximum coincidence window was 100 μs, which defined the maximum value of the bin array. All calculations were done with bins ranging from 1 - 30 μs. The justification behind this choice is discussed in the Changing Lifetime Array Length section; however, altering the size of the bin array does not have a significant effect on lifetime or $\tilde{\chi}^2$ (as seen in the Changing Maximum Lifetime Bin Number section).

The initial data and fit from September 1-6, 2022 are pictured in Figure 9. From the fit the $\tau = 2.095 \pm 0.034\,\mu s$. The initial lifetime and second lifetime (from Sept. 15-20) differ by 0.99%. The initial lifetime differs from literature muon lifetime by 4.6%. Again, the lower lifetime is most likely caused by the negative muon decays within the scintillator material.

5.1 Changing Bin Size

Changing the size of the bin can significantly alter the lifetime. The size of the bin was one of the choices made and was held consistent throughout the study. Until this point the bin size = 1 μs. To study the relationship between the lifetime and bin size, the analysis was executed with a bin size = 0.1, 0.2, 0.5, 1, 1.5, 2 and 4 μs. The results are plotting in Figure 10. The longest lifetime is 2.715 μs when bin size = 0.2 μs. The shortest lifetime is 2.108 μs which corresponds to a bin size of 1.5 μs. The lifetime for bin sizes of 0.2 and 1.5 μs differ from the literature value for lifetime by 23.6% and 4.05%, respectively. The difference between the longest and shortest lifetime is 28.8%. A bin size of 1, 1.5, 2 and 4 μs yield similar lifetimes. The error associated

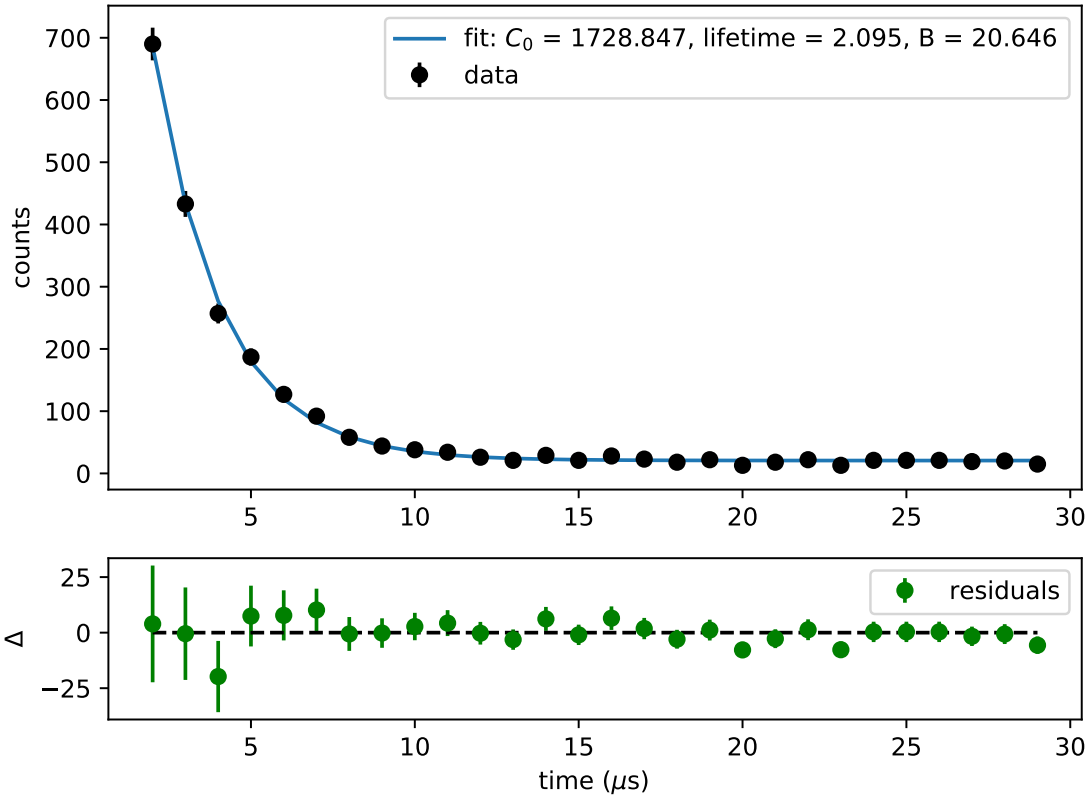

Figure 9: Same as Figure 6 but for the initial dataset collected September 1-6, 2022.

with bin size demonstrates the range of potential lifetimes controlled by a direct choice made during data analysis.

The $\tilde{\chi}^2$ value is plotted as a function of bin size. All $\tilde{\chi}^2$ values are on the order of one and indicate the fit is appropriate for the data regardless of bin size. The largest $\tilde{\chi}^2$ is 2.336 when bin size is equal to 0.5 μs. The smallest $\tilde{\chi}^2$ is 0.903 when bin size is 1.5 μs. For the smaller bin sizes, mainly 0.1 and 0.2, some bins had zero counts which meant dividing by zero in the $\tilde{\chi}^2$ calculation (equation 6). To avoid this issue, N_i and σ_i are set equal to 1, representing one standard deviation from zero counts for this bin.

5.2 Changing Maximum Lifetime Bin Number

The decision to limit bin range to 1 - 30 μs is based on Figure 11. This plot was constructed by restricting the maximum value included in the lifetime bin array to 15, 20, 30, 40, 50, 60, 70, 80, 90 and 100 μs. This limits the amount of background counts included in the fit. There are small variations in lifetime and $\tilde{\chi}^2$, as seen in Figure 11. The maximum lifetime occurs when bin array only includes lifetimes from 1 - 15 μs, with $\tau = 2.125$ μs. This differs from the accepted value by 3.3%. The smallest lifetime is calculated from the adjacent point with range 1-20 μs for a value of $\tau = 2.112$ μs. This differs from the literature value by 3.9%. The variation within points 1-30 μs (labeled as 30 μs) and 1-100 μs (labeled as 100 μs) is 0.28%. This is extremely small, indicating that setting the bin length array anywhere between 30 and 100 μs will yield similar lifetimes. Generally, the $\tilde{\chi}^2$ values decrease from 15 to 30 μs maximum bin, then remain relatively similar from 30 to 100 μs. The maximum $\tilde{\chi}^2$ value 2.01 and the minimum value

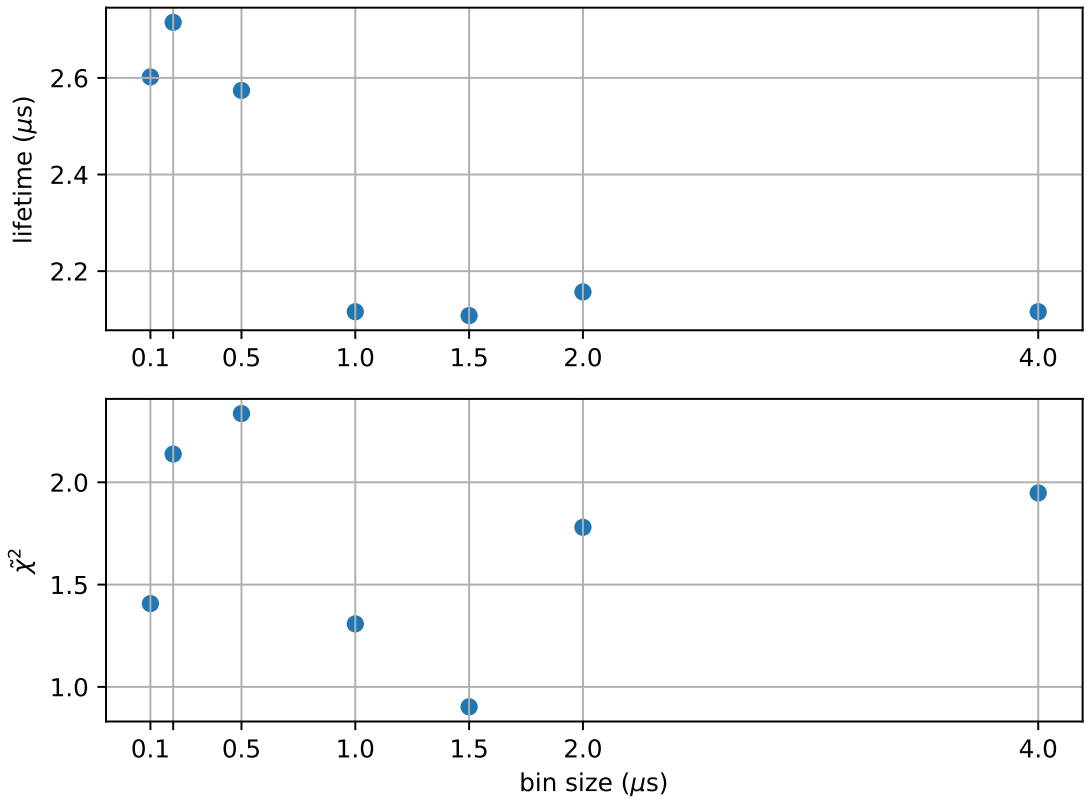

Figure 10: Plots showing dependence of lifetime and $\tilde{\chi}^2$ as a function of bin size specified. Bin sizes shown include 0.1, 0.2, 0.5, 1, 1.5 and 2 μs. The data plotted was collected from September 15-20, 2022.

1.08 occur at bin array size of 1-15 μs and 1-100 μs, respectively. Again, choosing a maximum lifetime bin array length between 30 and 100 μs will yield similar $\tilde{\chi}^2$ values. The range of $\tilde{\chi}^2$ all indicate an accurate fit for the dataset. In an effort to reduce computation time by limiting background points, a maximum lifetime bin array of 30 μs is sufficient.

6 Summary

Muons comprise the majority of cosmic ray particles reaching the surface of the earth. This study used a 15 cm x 10 cm x 12.6 cm scintillator, the CAEN DT5730S DAQ and external logic system to measure the lifetime of a muon. From the raw data, an exponential decay curve was constructed and fitted using non-linear least squares fitting method. The calculated muon lifetime from the fit $\tau = 2.116 \pm 0.027\,\mu s$. This differs from the literature value by 3.7% and these differences are attributed to the reduction of negative muon lifetime in carbon.

Independent statistic error analysis yield errors ranging from 0.020 μs to 0.034 μs. In addition, the choice of bin size and maximum lifetime bin number was explored and justified.

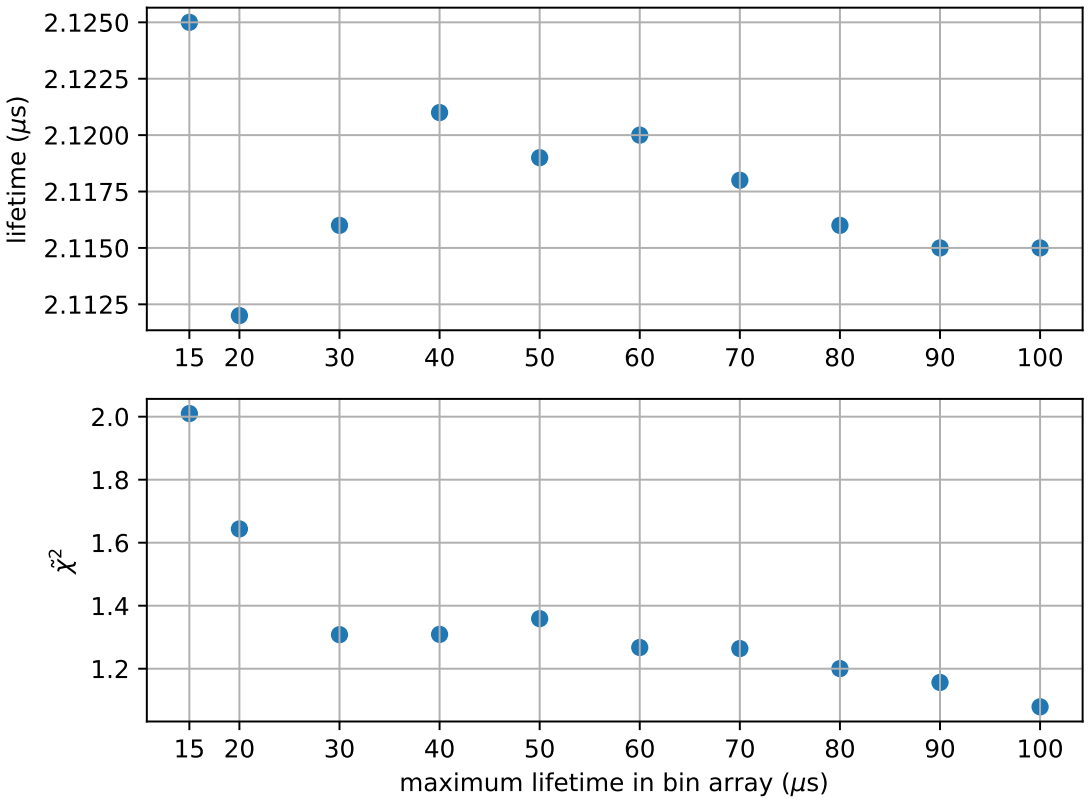

Figure 11: Plots showing dependence of lifetime and $\tilde{\chi}^2$ as a function of restricted lifetime bin array size. The maximum lifetime included in the bin array is indicated on the x-axis. The data plotted was collected from September 15-20, 2022.

References

M Bahmanabadi, MK Ghomi, and F Sheidaei. Experimental studies of positive and negative atmospheric muons with a cosmic rays telescope. *ASTROPARTICLE PHYSICS*, 24(3):183–190, OCT 2005. ISSN 0927-6505. doi: 10.1016/j.astropartphys.2005.06.005.

M. Bahmanabadi, F. Sheidaei, M. Khakian Ghomi, and J. Samimi. The charge ratio of the atmospheric muons at low energy. *PHYSICAL REVIEW D*, 74(8), OCT 2006. ISSN 1550-7998. doi: 10.1103/PhysRevD.74.082006.

V. Khachatryan and CMS Collaboration. Measurement of the charge ratio of atmospheric muons with the cms detector. *PHYSICS LETTERS B*, 692(2):83–104, AUG 23 2010. ISSN 0370-2693. doi: 10.1016/j.physletb.2010.07.033.

Y Kuno and Y Okada. Muon decay and physics beyond the standard model. *REVIEWS OF MODERN PHYSICS*, 73(1):151–202, JAN 2001. ISSN 0034-6861. doi: 10.1103/RevModPhys.73.151.

SH Neddermeyer and CD Anderson. Note on the nature of cosmic-ray particles. *PHYSICAL REVIEW*, 51(10):0884–0886, MAY 1937. ISSN 0031-899X. doi: 10.1103/PhysRev.51.884.